

Diversity-Multiplexing Tradeoff for Multi-Connectivity and the Gain of Joint Decoding

Albrecht Wolf, Philipp Schulz, David Öhmann, *Member, IEEE*,
Meik Dörpinghaus, *Member, IEEE*, and Gerhard Fettweis, *Fellow, IEEE*

Abstract

Multi-connectivity is considered to be key for enabling reliable transmissions and enhancing data rates in future wireless networks. In this work, we quantify the communication performance by the outage probability and the system throughput. We establish a remarkably simple, yet accurate analytical framework based on distributed source coding to describe the outage probability and the system throughput in dependency on the number of links, the modulation scheme, the code rate, the bandwidth, and the received signal-to-noise ratio (SNR). It is known that a tradeoff exists between the outage probability and the system throughput. To investigate this tradeoff we define two modes to either achieve low outage probabilities or high system throughput which we refer to as the diversity and the multiplexing mode, respectively. For the diversity mode, we compare three signal processing schemes and show the SNR gain of joint decoding in comparison to maximum selection combining and maximum ratio combining while achieving the same outage probability. We then establish a diversity-multiplexing tradeoff analysis based on time sharing between both modes. Additionally, we apply our analytical framework to real field channel measurements and thereby illustrate the potential of multi-connectivity in real cellular networks to achieve high reliability or high throughput.

Index Terms

Distributed source coding, diversity-multiplexing tradeoff, joint decoding, multi-connectivity, outage probability.

I. INTRODUCTION

Multi-connectivity (MC) is a promising concept for addressing the demand of high transmission reliability and high data rates in next generation wireless networks. However, a tradeoff exists between transmission reliability and data rates in any wireless communication system, including MC architectures. Motivated by this, we establish a diversity-multiplexing tradeoff analysis based on the relation of the outage probability and the system throughput for MC architectures. Furthermore, transmission reliability depends on the used signal processing scheme such as joint decoding (JD), maximum selection combining (MSC) and maximum ratio combining (MRC). To compare the performance of JD, MSC and MRC we derive their outage probabilities and thereby show the signal-to-noise-ratios (SNR) gain of JD in comparison to MSC and MRC while achieving the same outage probability. Next we briefly describe multi-connectivity, diversity-multiplexing tradeoff and joint decoding and then outline our approach and our contributions.

A. Multi-Connectivity

In wireless communications, MC concepts have been mainly developed and applied for increasing data rates and capacity. Various ways exist to realize MC, and we distinguish between two types, namely, intra- and inter-frequency MC. An overview of various techniques is given in Fig. 1. For instance, in case of intra-frequency MC in the downlink, multiple base stations (BSs) use the same carrier frequency to jointly transmit signals to a user. As a result, the received signal power and quality are improved, and diversity is facilitated. Established principles realizing intra-frequency MC are single frequency networks (SFN) [3] and coordinated multi-point (CoMP) [4], [5]. Another type of MC is inter-frequency MC, where a single or multiple BSs use multiple carrier frequencies to simultaneously transmit signals to a single user. In LTE, concepts such as carrier aggregation (CA) and dual connectivity (DC) have been introduced to make use of multiple so-called component carriers. CA and DC also support non-collocated deployments. As indicated before, existing realizations of MC are mainly used for enhancing data rates and capacities, i.e., different information is transmitted over each individual link (multiplexing). However, multiple connections can be also utilized to enhance the reliability, i.e., the same information is transmitted over all links in parallel (diversity). In

This work has been submitted to the IEEE for possible publication. Copyright may be transferred without notice, after which this version may no longer be accessible. The material in this work will be submitted in part to the IEEE GLOBECOM, Singapore, Dec., 2017, [1], [2].

The work of A. Wolf was supported by the Federal Ministry of Education and Research within the programme "Twenty20 - Partnership for Innovation" under contract 03ZZ0505B - "fast wireless". The work of M. Dörpinghaus was supported in part by the Deutsche Forschungsgemeinschaft (DFG) in the framework of the cluster of excellence EXC 1056 "Center for Advancing Electronics Dresden (cfaed)" and by the DFG within the Collaborative Research Center SFB 912 "Highly Adaptive Energy-Efficient Computing (HAEC)".

A. Wolf, P. Schulz, D. Öhmann, M. Dörpinghaus and G. Fettweis are with the Vodafone Chair Mobile Communications Systems, Technische Universität Dresden, Dresden, Germany, E-mails: {albrecht.wolf, philipp.schulz2, david.oehmann, meik.doerpinghaus, fettweis}@tu-dresden.de.

the context of ultra-reliable low latency communications (URLLC), MC is widely seen as a critical enabler of ultra-reliable connectivity, see e.g., [6]–[9].

Recently, research on URLLC is emerging considerably; nevertheless, there are only a few works focusing on a detailed

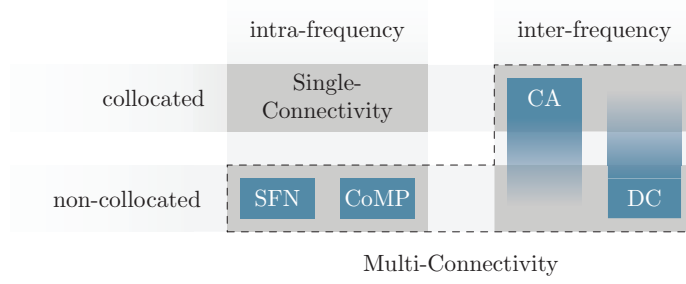


Fig. 1: Categorization of different MC architectures.

analysis of MC and its impact on reliability. In [6], [9], it is concluded that packet duplication across multiple connections is a suitable technique to achieve high reliability. Pocovi et al. evaluate intra-frequency MC in system simulations to illustrate how the SINR and the reliability is improved [10]. Furthermore, Tesema et al. demonstrate that mobility problems can be resolved by utilizing intra-frequency MC, see [11]. In another work by Nielsen and Popovski, multi-RAT architectures are compared regarding their latency, which is significantly improved by MC techniques [12].

B. Diversity-Multiplexing Tradeoff

In most wireless communication systems a demand for contradictory requirements exists: high transmission reliability and high data rates. In general, improving transmission reliability usually results in a decreased data rate, and vice versa. Therefore, it is crucial to balance these two contradictory requirements. Motivated by this, a fundamental diversity-multiplexing tradeoff (DMT) was first introduced by Zheng and Tse [13], [14], where the DMT is investigated for point-to-point multiple-input-multiple-output (MIMO) scenarios and multiple-access channels.

In [13], [14] the analyse is based on asymptotically large SNRs, which motivated Narasimhan to investigate more general and practical scenarios considering finite-SNR. In [15], a finite-SNR DMT for rate-adaptive MIMO systems was first defined and analyzed, which shows that for finite-SNR, the achievable diversity gains are significantly lower than in the asymptotic case. The finite-SNR DMT for relaying channels was further derived in [16].

In contrast to existing works, which focus on point-to-point MIMO channels, multiple-access channels and relaying channels, we investigate and model basic DMTs for MC, i.e., point-to-multipoint or multipoint-to-point systems.

C. Joint Decoding

In MC architectures signal processing schemes can be applied to increase transmission reliability. Several signal processing schemes are proposed, such as JD, MSC and MRC [17], [18]. In this work we concentrate on the analysis of JD, which can be established based on DSC. Slepian and Wolf [19] were the first to characterize the problem of distributed encoding of multiple correlated sources. In their seminal paper, the admissible rate region for the lossless distributed encoding of two correlated sources was derived. DSC can be used to analyze the performance of JD in MC architectures.

Motivated by the capabilities of JD Matsumoto et al. established an analytical framework to evaluate its performance. In [20], [21] the outage performance of JD was studied, based on DSC and the source-channel separation theorem [22, Theorem 3.7]. The outage probability of a decode-and-forward relaying system allowing intra-link errors (DF-IE) was derived in a classic three-node system model, i.e., one source, one relay and one destination. In [23] the system model was extended to an arbitrary number of relays and no direct links between source and destination. The outage probability is analytically described in dependency on the modulation scheme, the code rate, and the received SNR. A similar outage analysis can be established in the context of MC.

D. Problem Statement

Ultimately, network operators are interested in the quantitative relation between transmission reliability and data rates. Furthermore, the DMT depends on the applied signal processing schemes. As mentioned before different schemes are proposed in literature, namely, JD, MSC and MRC to achieve high transmission reliability. So far it is known that JD outperforms MSC and MRC but the gain cannot be quantified in terms of a transmission reliability parameter.

The aim is to find an analytical description of two parameters reflecting transmission reliability and data rates in the context of MC. A quantitative DMT analysis is of interest in dependency on the network configuration, the applied signal processing scheme and the physical layer design.

E. Contributions of this Work

We consider the MC architecture as a DSC setup, consisting of multiple correlated sources which are independently compressed at different terminals and the decoder aims to perfectly reproduce all sources. This allows us to use Slepian-Wolf's admissible rate region [19] which we adjust to the MC architecture. Based on the approach in [20], [21] we then derive the outage probability for JD, MSC and MRC. The outage probability is a quantitative parameter for transmission reliability. In addition, we define the system throughput as a quantitative parameter for data rates. Our diversity-multiplexing tradeoff analysis builds on the relation between outage probability and system throughput.

The contributions of this paper include the following:

- 1) We establish a remarkably simple, yet accurate analytical description of the outage probability and the system throughput for MC architectures based on DSC. We consider two modes, i.e., either the same information is transmitted over multiple communication links, which we refer to as the diversity mode, or different information is transmitted over the communications links, which we refer to as the multiplexing mode. For both modes the outage probability and the system throughput are analytically described in dependency on the number of links, the modulation scheme, the code rate, the bandwidth, and the received SNR. In other words, we derive a theoretical framework for analyzing wireless connectivity. The framework helps avoiding extensive system simulations.
- 2) For the diversity mode we compare three different signal processing schemes, namely, JD, MSC and MRC. We show the SNR gain of JD in comparison to MSC and MRC while achieving the same outage probability.
- 3) We establish a diversity-multiplexing tradeoff by the time sharing argument, i.e., time sharing of the communication link resources between the diversity and multiplexing mode. Time sharing enables a simple characterization although not necessarily being optimal. The diversity-multiplexing tradeoff allows us to understand the relation between high throughput and high reliability in the MC context. Considering a wireless network, our diversity-multiplexing tradeoff analysis allows the network to accurately adjust the system configurations, in dependency on the user requirements,
- 4) Finally, we apply our framework to real field channel measurements and thereby show the potential of MC in real cellular networks to achieve high reliability or high throughput.

F. Notation and Terminology

The upper- and lowercase letters are used to denote random variables (RVs) and their realizations, respectively, unless stated otherwise. The alphabet set of a random variable X with realization x is denoted by \mathcal{X} , and its cardinality, respectively by $|\mathcal{X}|$. The probability mass function (pmf)/probability density function (pdf) of the discrete/continuous random variable X is denoted by $p_X(x)/f_X(x)$, or simply $p(x)/f(x)$ when this does not create any confusion. Also, \mathbf{X} and \mathbf{x} represent vectors containing a temporal sequence of X and x , respectively. All random vectors have length n (block length) if not stated otherwise. We use k to denote the time index and i to denote a source index. We define $\mathbf{A}_S = \{\mathbf{A}_i | i \in S\}$ as an indexed series of random vectors, and $A_S = \{A_i | i \in S\}$ as an indexed series of random variables. In general, a set \mathbf{A} contains elements $a_{(\cdot)}$, as in $\mathbf{A} = \{a_1, a_2, \dots, a_{|\mathbf{A}|}\}$. We define one particular set: $\mathcal{N} = \{1, 2, \dots, N\}$. We denote the Laplace transform of $f(x)$ as $\mathcal{L}_x[f(x)](p)$, the probability of an event \mathcal{E} as $\Pr[\mathcal{E}]$, and the convolution as $*$.

II. SYSTEM MODEL

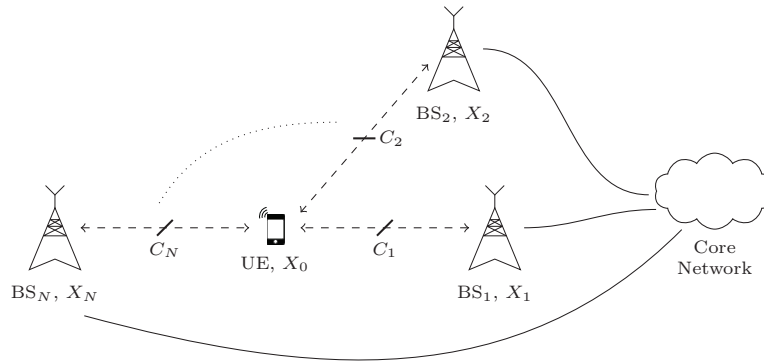


Fig. 2: System model with a single UE, N base stations, and a core network.

A. Multi-Connectivity System Model

We consider a MC cellular network, as shown in Fig. 2, consisting of a core network, N base stations ($\text{BS}_i, \forall i \in \mathcal{N}$), communicating to a single user equipment (UE). The core network coordinates the data transmissions to the UE. Connections between the core network and each BS are realized by backhaul links, and connections between each BS and UE by wireless links. The achievable transmission rate over the i th wireless link depends on its capacity C_i . In the system model, we distinguish between down- and uplink. In the downlink, N BSs transmit data to one UE whereas in the uplink one UE transmits data to N BSs. This difference has implications on the system model as we explain in detail now.

a) Downlink: The downlink system model has N binary memoryless sources (in this mode we refer to a BS as source), denoted as $\{(X_{1,k}, X_{2,k}, \dots, X_{N,k})\}_{k=1}^{\infty}$, with the n -sample sequence of the i th source being represented in vector form as $\mathbf{X}_i = [X_{i,1}, X_{i,2}, \dots, X_{i,n}]$, $\forall i \in \mathcal{N}$. When appropriate, for simplicity, we shall drop the temporal index of the sequences, denoting the sources merely as X_1, X_2, \dots, X_N . By assumption, X_1, X_2, \dots, X_N take values in binary sets $\mathcal{X}_i = \{0, 1\}$ with uniform probabilities, i.e., $\Pr[X_i = 0] = \Pr[X_i = 1] = 0.5, \forall i \in \mathcal{N}$. Each source sequence \mathbf{X}_i is encoded, modulated and transmitted to the destination (in this mode we refer to the UE as destination). The communication links use multiple frequencies, which are separated by the coherence bandwidth, to transmit the information. Thus, the communication links are assumed to be uncorrelated [24], cf. Section II-B. At the destination, we have two decoding strategies in dependency on the mode.

- *Diversity mode:* If the sources X_1, X_2, \dots, X_N are identical, JD is performed at the destination to retrieve them. JD can exploit the correlation of the received sequences. The entropy of all sources is

$$H(X_N) = H(X_i) = 1. \quad (1)$$

- *Multiplexing mode:* If the sources X_1, X_2, \dots, X_N are independent, each received sequence is decoded individually at the destination to retrieve them. The entropy of all sources is

$$H(X_N) = NH(X_i) = N. \quad (2)$$

Remark: In (1) and (2) we merely consider corner cases of the entropy of all sequences $H(X_N)$. In dependency on the joint pmf $p(x_N)$ the entropy can take values between $1 \leq H(X_N) \leq N$. In Section VII we elaborate on this in detail. For the outage analysis we solely consider both corner cases.

b) Uplink: The uplink system model has one binary memoryless source (in this mode we refer to the UE as source), denoted as $\{X_{0,k}\}_{k=1}^{\infty}$, with the n -sample sequence of the source being represented in vector form as $\mathbf{X}_0 = [X_{0,1}, X_{0,2}, \dots, X_{0,n}]$. By assumption, X_0 takes values in a binary set $\mathcal{X}_0 = \{0, 1\}$ with uniform probabilities, i.e., $\Pr[X_0 = 0] = \Pr[X_0 = 1] = 0.5$. The source sequence \mathbf{X}_0 is encoded, modulated and transmitted to all BSs. All received sequences are forwarded to the core network and jointly decoded to retrieve \mathbf{X}_0 (in this mode we refer to all BSs and core network as destination). The joint decoder can exploit the correlation of the received sequences. The entropy of the source is

$$H(X_0) = 1. \quad (3)$$

Naturally, we cannot establish a multiplexing mode for the uplink, since there is only a single source.

B. Link Model

Instead of sending multiple sequences at different time instances, i.e., coding in time, we use multiple frequency channels to transmit the information. Thus, the information can, in the best case, be delivered in a single time slot, which helps satisfying the URLLC requirements. The frequency channels can be realized by using different channels within a single frequency band or, alternatively, by using channels of different frequency bands, c.f. inter-frequency MC in Section I. According to [24], the small-scale fading of two signals is approximately uncorrelated if their frequencies are at least separated by the coherence bandwidth, which is confirmed, for instance, by measurement results in [25]. In the following, we assume that the used frequency resources are at least separated by the coherence bandwidth. Thus, the channels are uncorrelated. Furthermore, to cope with the low latency constraint in URLLC, we consider relatively short encoded sequences. As a result, the length of a encoded sequence is less or equal to the length of a fading block of the block Rayleigh fading. Moreover, the signals are transmitted from or to different BSs, which leads to individual average SNR values.

As argued, we can assume that the sequences are transmitted (up- and downlink) over independent channels undergoing block Rayleigh fading and additive white Gaussian noise (AWGN) with mean power N_0 . The pdf of the received SNR Γ_i is given by

$$f_{\Gamma_i}(\gamma_i) = \frac{1}{\bar{\Gamma}_i} \exp\left(-\frac{\gamma_i}{\bar{\Gamma}_i}\right), \quad (4)$$

with the average SNR $\bar{\Gamma}_i$ being obtained as

$$\bar{\Gamma}_i = \frac{P_i}{N_0} \cdot d_i^{-\eta}, \quad (5)$$

where P_i is the transmit power of BS_i , P_0 is the transmit power of the UE, d_i is the distance between BS_i and the UE, and η is the path loss exponent. The channel state information is known at the receiver.

For the downlink, we introduce a total amount of transmit power P_T which is equally allocated at all BSs, thus the transmit power at the i th BS is assigned as $P_i = 1/N P_T, \forall i \in \mathcal{N}$. Then, from (5), the downlink average received SNR at the destination can be written as

$$\bar{\Gamma}_i = \frac{1/N P_T}{N_0} \cdot d_i^{-\eta}. \quad (6)$$

In addition, we define the average system transmit SNR as P_T/N_0 in dB, i.e., normalizing all distances d_i to one. We shall use a total transmit power constraint for comparison of different configurations later on.

Remark: In the following we merely consider the downlink. However, the results for the uplink are similar to the downlink diversity mode. We will discuss the uplink in Section IX.

III. PRELIMINARIES

In this section, we outline how we connect DSC to the outage analysis of the MC system model. First, we recall fundamentals on the source-coding separation theorem; second, we recall the Slepian-Wolf admissible rate region, which will then be adjusted to the MC system model; and third, we illustrate the mapping of the admissible rate region into an admissible SNR region.

A. Source-Channel Separation Theorem

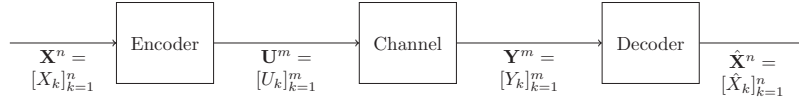


Fig. 3: Joint source-channel coding setup.

Fig. 3 illustrates a joint source-channel (JSC) setup. The encoder sends a codeword $\mathbf{U}^m \in \mathcal{U}^m$ for the source samples $\mathbf{X}^n \in \mathcal{X}^n$, and the decoder generates an estimate $\hat{\mathbf{X}}^n$ based on the received sequence \mathbf{Y}^m . A prevalent way, in this case, is to perform source and channel encoding as well as channel and source decoding separately. For the point-to-point communication with memoryless source and memoryless channels, Shannon proved that such strategy is asymptotically optimal, i.e., $n \rightarrow \infty$, which is called Shannon's source-channel separation theorem.

Theorem 1 (Source-channel separation theorem [22, Theorem 3.7]) *Given a discrete memoryless source X , an average distortion measure $d(x, \hat{x})$ with rate-distortion function $R(D)$ and a discrete memoryless channel with capacity C , the following statement holds.*

If $nR(D) \leq mC$, then there exists a sequence of JSC codes such that

$$\limsup_{n \rightarrow \infty} \mathbb{E} [d(\mathbf{X}^n, \hat{\mathbf{X}}^n)] \leq D, \quad (7)$$

where n is the number of source samples and m is the number of channel symbols. $R(D)$ is expressed in bits per sample and the capacity C is in bits per channel symbol.

For more details on this JSC coding setup, please refer to [26, Section 2].

B. Slepian-Wolf Theorem

Slepian and Wolf [19] considered a source coding problem where the decoder aims at perfectly reproducing two correlated sources, which are independently compressed at two terminals. In their seminal paper, the admissible rate region for this problem was derived. A simple proof of the Slepian-Wolf result with extension to an arbitrary number of correlated sources was presented by Cover in [27].

Theorem 2 (Generalized Slepian-Wolf theorem [27]) *In order to achieve lossless compression of N correlated sources X_1, X_2, \dots, X_N , the source code rates $R_i, \forall i \in \mathcal{N}$, measured in bits per sample, should satisfy the following conditions*

$$\sum_{i \in \mathcal{S}} R_i \geq H(\{X_i | i \in \mathcal{S}\} | \{X_j | j \in \mathcal{S}^c\}), \forall \mathcal{S} \subseteq \mathcal{N}, \quad (8)$$

where \mathcal{S}^c denotes the complement of \mathcal{S} .

The set of N -tuples R_1, \dots, R_N that satisfy all the constraints in (8) is referred to as the Slepian-Wolf admissible rate region \mathcal{R}_{SW} .

With the assumption on the entropy of the diversity mode in (1), i.e., N identical sources X_1, X_2, \dots, X_N , the Slepian-Wolf admissible rate region in (8) simplifies to

$$\sum_{i=1}^N R_i \geq H(X_i) = 1 \quad (9)$$

The set of N -tuples R_1, \dots, R_N that satisfy all the constraints in (9) is referred to as the MC-diversity admissible rate region $\mathcal{R}_{\text{MC-D}}$.

As JD is not applied for the multiplexing mode, lossless compression of source X_i , can be achieved if the source code rate R_i satisfies the following condition, see, e.g., [28, Theorem 10.3.1]

$$R_i \geq H(X_i) = 1. \quad (10)$$

C. Mapping: SNR to Rate

According to [22, Theorem 3.7], [21] the maximum achievable value of the transmission rate R_i is then related to the received SNR Γ_i , based on the block Rayleigh fading assumption, by

$$R_i = \frac{1}{n/m} C(\Gamma_i) = \frac{1}{R_{i,c}} \phi(\Gamma_i), \quad (11)$$

where $\phi(\Gamma_i) = \log_2(1 + \Gamma_i)$, $R_{i,c}$ represents the spectral efficiency, measured in samples per channel symbol, associated with the modulation scheme $R_{i,M} = \log_2(M)$, the cardinality of the channel symbol alphabet M and the channel code rate $R_{i,\text{cod}}$, i.e., $R_{i,c} = R_{i,M} \cdot R_{i,\text{cod}}$. If not otherwise stated, for simplicity, we shall assume $R_{i,c} = R_c$. For more details on this SNR to rate mapping, please refer to [21].

Fig. 4 illustrates the diversity mode's SNR to rate mapping for $N = 2$. Lets assume that we have two received SNR realizations, i.e., 2-tuple (γ_1, γ_2) . With (11) we can map the received SNR realizations into the transmission rate domain, i.e., 2-tuple $(1/R_c \cdot \phi(\gamma_1), 1/R_c \cdot \phi(\gamma_2))$. In Fig. 4 we illustrated two different 2-tuples at point A and point B . In addition, Fig. 4 illustrates the MC-diversity admissible rate region $\mathcal{R}_{\text{MC-D}}$ and its counterpart the MC-diversity inadmissible rate region $\mathcal{R}_{\text{MC-D}}^c$. Both regions are separated from each other by the rate constraint in (9), i.e., $R_1 + R_2 = 1$. For the multiplexing mode, the

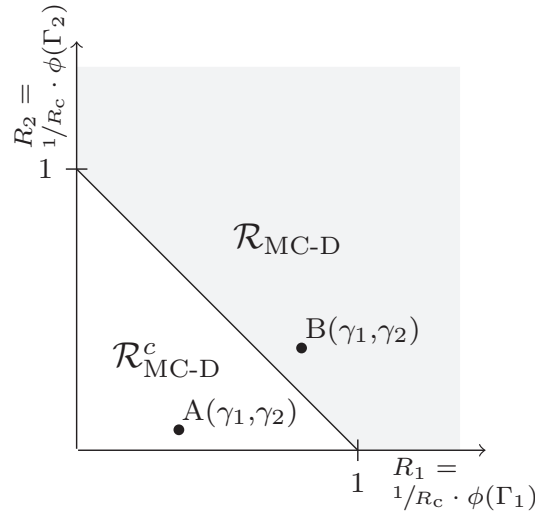


Fig. 4: MC-diversity admissible rate region and SNR to rate mapping.

SNR to rate mapping is identical, but each transmission rate is considered individually. The received SNR realization γ_i can be mapped with (11) into the transmission rate domain, i.e., $1/R_c \cdot \phi(\gamma_i)$.

IV. OUTAGE PROBABILITY

In the diversity mode, an outage event occurs whenever the transmission rate N -tuple R_1, \dots, R_N fall outside the MC-diversity admissible rate region $\mathcal{R}_{\text{MC-D}}$. Using (11), the sum rate constraint in (9) that defines $\mathcal{R}_{\text{MC-D}}$ can be mapped into a set of equivalent SNR constraints. Fig. 4 illustrates this approach for $N = 2$. The received SNR realizations, i.e., 2-tuple (γ_1, γ_2) , at point A , are transformed into transmission rates, i.e., 2-tuple $(1/R_c \cdot \phi(\gamma_1), 1/R_c \cdot \phi(\gamma_2))$. Since the transmission rate 2-tuple

at point A is outside the MC-diversity admissible rate region $\mathcal{R}_{\text{MC-D}}$ an outage event occurs, i.e., the joint decoder cannot perfectly reproduce the source sequence $\mathbf{X}_i, \forall i \in \mathcal{N}$. The transmission rate 2-tuple at point B is inside the MC-diversity admissible rate region $\mathcal{R}_{\text{MC-D}}$, i.e., the joint decoder can perfectly reproduce the source sequence $\mathbf{X}_i, \forall i \in \mathcal{N}$.

In the multiplexing mode, an outage event of the i th source occurs whenever the transmission rate R_i does not satisfy the rate constraint in (10), i.e., the decoder cannot perfectly reproduce the source sequence \mathbf{X}_i .

In this section, we aim to derive an exact integral-form for the outage probability based on the MC-diversity admissible rate region. We distinguish between the diversity and the multiplexing mode. For the diversity mode, we establish the exact outage probability in integral-form. Unfortunately, the integral-form cannot be solved in closed-form, thus we give an approximation for the high SNR regime. For the multiplexing mode we establish the exact outage probability in closed-form.

A. Outage Probability for the Diversity Mode

As discussed before, an outage occurs if the transmission rate N -tuple R_1, \dots, R_N falls outside the MC-diversity admissible rate region $\mathcal{R}_{\text{MC-D}}$, i.e., (9) is not fulfilled. Thus the outage probability for the diversity mode can be calculated as follows:

$$P_{\text{D},N}^{\text{out}} = \Pr[0 \leq R_1 + R_2 + \dots + R_N < 1] \quad (12)$$

$$= \Pr[0 \leq \phi(\Gamma_1) + \phi(\Gamma_2) + \dots + \phi(\Gamma_N) < R_c] \quad (13)$$

$$= \Pr[0 \leq \phi(\Gamma_1) < R_c, 0 \leq \phi(\Gamma_2) < R_c - \phi(\Gamma_1), \dots, \\ 0 \leq \phi(\Gamma_N) < R_c - \phi(\Gamma_1) - \phi(\Gamma_2) - \dots - \phi(\Gamma_{N-1})] \quad (14)$$

$$= \Pr\left[0 \leq \Gamma_1 < 2^{R_c} - 1, 0 \leq \Gamma_2 < 2^{R_c - \phi(\Gamma_1)} - 1, \dots, \right. \\ \left. 0 \leq \Gamma_N < 2^{R_c - \phi(\Gamma_1) - \phi(\Gamma_2) - \dots - \phi(\Gamma_{N-1})} - 1\right] \quad (15)$$

$$= \int_{\gamma_1=0}^{2^{R_c}-1} \int_{\gamma_2=0}^{2^{R_c-\phi(\gamma_1)}-1} \dots \int_{\gamma_N=0}^{2^{R_c-\phi(\gamma_1)-\phi(\gamma_2)-\dots-\phi(\gamma_{N-1})}-1} \\ f(\gamma_1)f(\gamma_2)\dots f(\gamma_N)d\gamma_N\dots d\gamma_2d\gamma_1. \quad (16)$$

The steps are justified as follows: (12) is the constraint on the sum rate in (9); in (13) the rate constraint is mapped into the SNR constraint with use of (11); in (14) the sum constraint is separated into individual constraints; in (15) the bounds are transformed with $\phi^{-1}(y) = 2^y - 1$; in (16) the probability of outage is established in integral-form with the assumption that the received SNRs are independent. The pdf $f(\gamma_i)$ is given in (4). Although the outage expression in (16) cannot be solved in closed-form, a simple asymptotic solution can be derived at high SNR

$$P_{\text{D},N}^{\text{out}} \approx \int_{\gamma_1=0}^{2^{R_c}-1} \int_{\gamma_2=0}^{2^{R_c-\phi(\gamma_1)}-1} \dots \int_{\gamma_N=0}^{2^{R_c-\phi(\gamma_1)-\phi(\gamma_2)-\dots-\phi(\gamma_{N-1})}-1} \\ \frac{1}{\bar{\Gamma}_1\bar{\Gamma}_2\dots\bar{\Gamma}_N}d\gamma_N\dots d\gamma_2d\gamma_1 \quad (17)$$

$$= \frac{A_N}{\bar{\Gamma}_1\bar{\Gamma}_2\dots\bar{\Gamma}_N} \quad (18)$$

where

$$A_N = (-1)^N + 2^{R_c} \sum_{n=0}^{N-1} (-1)^{N+n+1} \frac{1}{n!} R_c^n (\ln(2))^n. \quad (19)$$

For more details, we refer to the derivations in Appendix A. It holds that $\partial A_N / \partial R_c > 0$. The spectral efficiency is associated with the modulation scheme and the channel code rate, i.e., $R_{i,c} = R_{i,M} \cdot R_{i,\text{cod}}$. Generally speaking, if the modulation order increases while the code rate stays constant, the constant A_N increases as well. If the code rate increases while the modulation order stays constant, the constant A_N increases as well. Since $P_{\text{D},N}^{\text{out}} \sim A_N$ as given in (18), the relation between $P_{\text{D},N}^{\text{out}}$ and R_c is reasonable. We will discuss the outage probability $P_{\text{D},N}^{\text{out}}$ based on numerical examples in Section VIII.

B. Outage Probability for the Multiplexing Mode

As discussed before, an outage event of the i th source occurs whenever the transmission rate R_i does not satisfy the rate constraint in (10). Thus the outage probability of the i th source can be calculated as follows:

$$P_{\text{M},i}^{\text{out}} = \Pr[0 \leq R_i < 1] \quad (20)$$

$$= \Pr[0 \leq \phi(\Gamma_i) < R_c] \quad (21)$$

$$= \Pr[0 \leq \Gamma_i < 2^{R_c} - 1] \quad (22)$$

$$= \int_{\gamma_i=0}^{2^{R_c}-1} f(\gamma_i)d\gamma_i \quad (23)$$

$$= 1 - \exp\left(-\frac{A_1}{\Gamma_i}\right) \quad (24)$$

with $A_1 = 2^{R_c} - 1$. The steps are justified as follows: (20) is the constraint on the rate in (10); (21) - (23) follow the same arguments as in (13), (15), and (16), respectively; (24) is the closed-form solution of the integral in (23). In the diversity mode the communication link resources are used N times to transmit the information rate $H(X_{\mathcal{N}}) = 1$. In the multiplexing mode the communication link resources are used N times to transmit the information rate $H(X_{\mathcal{N}}) = N$. To make a fair comparison to the diversity mode, we define the outage probability of the multiplexing mode $P_{M,N}^{\text{out}}$ by averaging over all outage probabilities $P_{M,i}^{\text{out}}$ and thus normalize the multiplexing mode information rate.

$$P_{M,N}^{\text{out}} = \frac{1}{N} \sum_{i=1}^N P_{M,i}^{\text{out}} \quad (25)$$

$$= \frac{1}{N} \sum_{i=1}^N \left(1 - \exp\left(-\frac{A_1}{\Gamma_i}\right)\right) \quad (26)$$

We will discuss the outage probability $P_{M,N}^{\text{out}}$ based on numerical examples in Section VIII.

V. SUBOPTIMAL SCHEMES FOR DIVERSITY MODE

In this section, we consider two additional signal processing schemes for the diversity mode, namely MSC and MRC. Both schemes are known to be suboptimal in comparison to the JD scheme [17]. We aim to quantify this qualitative statement in terms of SNR reduction while achieving the same outage probability in the MC context.

A. Outage Probability for Maximum Selection Combining

For MSC [18] at each time instant only the channel with the maximum transmission rate $R_{\max} = \max(R_1, R_2, \dots, R_N)$ is selected. If R_{\max} does not satisfy the rate constraint in (10) an outage occurs. In other word, each received source sequence is decoded individually and no received source sequence can be perfectly reproduce.

$$P_{\text{MSC},N}^{\text{out}} = \Pr[0 \leq R_{\max} < 1] \quad (27)$$

$$= \Pr[0 \leq \phi(\Gamma_{\max}) < R_c] \quad (28)$$

$$= \Pr[0 \leq \phi(\Gamma_1) < R_c, 0 \leq \phi(\Gamma_2) < R_c, \dots, 0 \leq \phi(\Gamma_N) < R_c] \quad (29)$$

$$= \Pr[0 \leq \Gamma_1 < 2^{R_c} - 1, 0 \leq \Gamma_2 < 2^{R_c} - 1, \dots, 0 \leq \Gamma_N < 2^{R_c} - 1] \quad (30)$$

$$= \prod_{i=1}^N \int_{\gamma_i=0}^{2^{R_c}-1} f(\gamma_i) d\gamma_i \quad (31)$$

$$= \prod_{i=1}^N \left(1 - \exp\left(-\frac{A_1}{\Gamma_i}\right)\right) \quad (32)$$

The steps can be justified similar to (20) - (24). In (31) the multiple integral can be rewritten as the product of single integrals, since the integral bounds in (30) are independent.

B. Outage Probability for Maximum Ratio Combining

For MRC [18] all received symbols are coherently added. The sum of all symbols is then decoded. We can apply the point-to-point communication system assumption in Section III-A if we define an auxiliary RV, namely the total received SNR Γ_{MRC} as

$$\Gamma_{\text{MRC}} = \sum_{i=1}^N \Gamma_i. \quad (33)$$

The pdf of the received SNR Γ_{MRC} is given by

$$f_{\Gamma_{\text{MRC}}}(\gamma_{\text{MRC}}) = f_{\Gamma_1}(\gamma_1) * f_{\Gamma_2}(\gamma_2) * \dots * f_{\Gamma_N}(\gamma_N) \quad (34)$$

$$= \mathcal{L}_p^{-1}[\mathcal{L}_{\gamma_1}[f_{\Gamma_1}(\gamma_1)](p) \cdot \mathcal{L}_{\gamma_2}[f_{\Gamma_2}(\gamma_2)](p) \cdot \dots \cdot \mathcal{L}_{\gamma_N}[f_{\Gamma_N}(\gamma_N)](p)](\gamma_{\text{MRC}}) \quad (35)$$

$$= \frac{\gamma_{\text{MRC}}^{(N-1)}}{(N-1)! \cdot \Gamma_i^N} \exp\left(-\frac{\gamma_{\text{MRC}}}{\Gamma_i}\right) \quad (36)$$

The steps are justified as follows: for (34) the pdf of a sum of RVs is the convolution of their pdfs; for (35) a convolution of functions is a multiplication of their Laplace transforms where $\mathcal{L}_{\gamma_i}[f_{\Gamma_i}(\gamma_i)](p) = 1/(\Gamma_i p + 1)$. The result in (36) holds for

$\bar{\Gamma}_1 = \dots = \bar{\Gamma}_N = \bar{\Gamma}_i$ which we assume for simplicity. With the total received SNR Γ_{MRC} we can assume a point-to-point communication system and thus the outage probability can be calculated as follows:

$$P_{\text{MRC},N}^{\text{out}} = \Pr[0 \leq R_{\text{MRC}} < 1] \quad (37)$$

$$= \Pr[0 \leq \phi(\Gamma_{\text{MRC}}) < R_c] \quad (38)$$

$$= \Pr[0 \leq \Gamma_{\text{MRC}} < 2^{R_c} - 1] \quad (39)$$

$$= \int_{\gamma_{\text{MRC}}=0}^{2^{R_c}-1} f(\gamma_{\text{MRC}}) d\gamma_{\text{MRC}}. \quad (40)$$

$$= 1 - \exp\left(-\frac{A_1}{\bar{\Gamma}_i}\right) \left(\sum_{i=1}^N \frac{(A_1/\bar{\Gamma}_i)^{(i-1)}}{(i-1)!}\right) \quad (41)$$

The steps can be justified similar to (20) - (23). The closed-form of the integral in (40) is given in [29, (2.33)].

C. Performance Comparison

To quantify the performance gain of JD in comparison to MSC and MRC in terms of the outage probability, we evaluate the average system transmit SNR P_T/N_0 in (6) to achieve a target outage probability P_*^{out} . Thus we substituted (6) into (18), (32) and (41) for JD, MSC and MRC, respectively, yielding

$$\frac{P_T}{N_0} = \sigma_i(P_*^{\text{out}}), \quad (42)$$

where $\sigma_i(P_*^{\text{out}})$ is the required average system transmit SNR depending on P_*^{out} and the signal processing scheme, $i \in \{\text{JD}, \text{MSC}, \text{MRC}\}$. In order to examine the SNR gain provided by JD versus MRC and MRC, we consider the reduction of the required average system transmit SNR while achieving the same target outage probability. The SNR gain is given by

$$G_{\text{JD},i} = \frac{\sigma_i(P_*^{\text{out}})}{\sigma_{\text{JD}}(P_*^{\text{out}})} \quad (43)$$

for $i \in \{\text{MSC}, \text{MRC}\}$. We will discuss the performance comparison based on numerical examples in Section VIII.

VI. SYSTEM THROUGHPUT

Although the outage probability is an effective measure for the likelihood that each transmission succeeds, it does not capture how much information the destination receives on average per transmission. To capture this, following the standard approach in literature [17], we define the system throughput T as the product of the bandwidth B , spectrum efficiency R_c , entropy of all sequences $H(X_N)$ and the non-outage probability $(1 - P_{\text{D},N}^{\text{out}}(R_c, \bar{\Gamma}_N))$, which gives

$$T_{\text{D},N}(B, R_c, \bar{\Gamma}_N) = B \cdot R_c \cdot H(X_N) \cdot (1 - P_{\text{D},N}^{\text{out}}(R_c, \bar{\Gamma}_N)) \text{ in bit/s}, \quad (44)$$

The outage probability $P_{\text{D},N}^{\text{out}}$ can be computed by using the mathematical framework developed heretofore and depends on the mode, the number of BSs N , the average SNR $\bar{\Gamma}_N$, and the spectral efficiency R_c . The bandwidth and spectral efficiency are parameters which are given by the physical layer components. Similar as for the outage probability we distinguish between the diversity and multiplexing mode.

- *Diversity mode:* The diversity mode system throughput can be calculated by replacing $H(X_N)$ with (1) and substituting (16) into (44) to

$$T_{\text{D},N} = B \cdot R_c \cdot (1 - P_{\text{D},N}^{\text{out}}) \text{ in bit/s}, \quad (45)$$

and approximated with (18) by

$$T_{\text{D},N} \approx B \cdot R_c \cdot \left(1 - \frac{A_N}{\bar{\Gamma}_1 \bar{\Gamma}_2 \dots \bar{\Gamma}_N}\right) \text{ in bit/s} \quad (46)$$

- *Multiplexing mode:* The multiplexing mode system throughput can be calculated by replacing $H(X_N)$ with (2) and substituting (26) into (44) to

$$T_{\text{M},N} = B \cdot R_c \cdot N \cdot \left(1 - \frac{1}{N} \sum_{i=1}^N \left(1 - \exp\left(-\frac{2^{R_c}-1}{\bar{\Gamma}_i}\right)\right)\right) \text{ in bit/s}. \quad (47)$$

VII. TRADEOFF BETWEEN THROUGHPUT AND OUTAGE

The outage probability and the system throughput are inherently connected. Both parameters depend on the mode as pointed out in Section IV and Section VI. In the diversity mode a low outage probability can be achieved at the cost of a low system throughput and vice versa for the multiplexing mode. As pointed out in Section II-A, we only consider corner cases of the entropy of all sequences, i.e., $H(X_N) = 1$ or N , with the diversity mode and multiplexing mode introduced before so far. However, $H(X_N)$ can take any value between these corner cases. In the following, we establish a DMT to account for all values of $H(X_N)$.

A. Time Sharing

We can achieve any value of $H(X_N) = \alpha + (1 - \alpha) \cdot N$ by the time sharing argument, i.e., both modes are in operation for a certain time interval. The parameter $\alpha \in [0, 1]$ allocates the time share for both modes accordingly. Thus the outage probability is defined as

$$P_N^{\text{out}} = \alpha \cdot P_{D,N}^{\text{out}} + (1 - \alpha) \cdot P_{M,N}^{\text{out}}. \quad (48)$$

Similar to the outage probability the system throughput is defined as

$$T_N = \alpha \cdot T_{D,N} + (1 - \alpha) \cdot T_{M,N}. \quad (49)$$

Remark: Time sharing enables a simple characterization of the DMT analysis but is not necessarily the optimal scheme.

B. Diversity-Multiplexing Tradeoff

To achieve a fair tradeoff analysis, we make use of the total transmit power constraint in (6). Then, the outage probability can be given as a function of α and P_T , defined as $P_N^{\text{out}} = g_{P_N^{\text{out}}}(\alpha, P_T)$, i.e., substitute (6) into (48). The system throughput can be given as a function of α and P_T , defined as $T_N = g_{T_N}(\alpha, P_T)$, i.e., substitute (6) into (49). Finally, we establish the DMT by the stationary curve for $0 \leq \alpha \leq 1$ as

$$(P_N^{\text{out}}, T_N) = (g_{P_N^{\text{out}}}(\alpha, P_T), g_{T_N}(\alpha, P_T)). \quad (50)$$

We will discuss the DMT based on numerical examples in Section VIII.

VIII. NUMERICAL RESULTS

In this section we illustrate and discuss the outage probability and system throughput in different scenarios. In each scenario, the outage probability and system throughput are assessed in an asymptotic fashion, as well as via Monte-Carlo integration (diversity mode) or an analytical solution (multiplexing mode). For illustration purpose, we assume a binary phase-shift keying modulation and a channel-code rate of $1/2$, so that $R_c = 0.5$. Moreover, we assume a path loss exponent of $\eta = 3.5$, and a bandwidth of $B = 20$ MHz. We consider N BSs, where we show results for $N = 1, \dots, 10$. To ensure a fair comparison of different modes, we make use of the total transmit power constraint in (6), i.e., the transmit power is equally allocated to all BSs, $P_i = P_T/N$.

Fig. 5a depicts the exact and approximated outage probability $P_{D,N}^{\text{out}}$ for the diversity mode in (16) and (18), respectively,

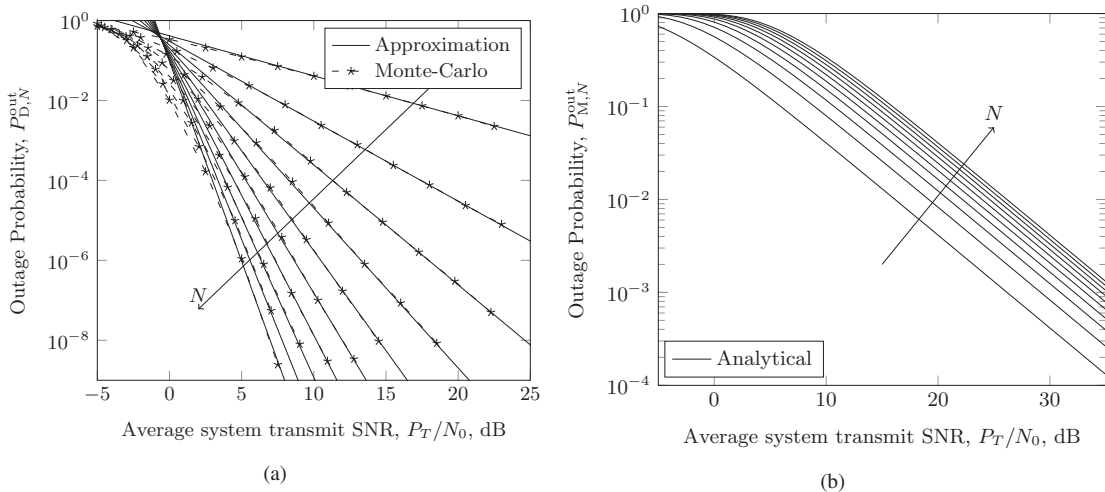


Fig. 5: Exact and approximated outage probability with $N = 1, 2, \dots, 10$ for (a) diversity mode and (b) multiplexing mode.

versus the average system transmit SNR P_T/N_0 . We show results for different numbers of BSs. The following can be observed: (i) our asymptotic expression in (18) is tight at medium to high SNR; and (ii) with every additional BS the diversity order [17] increases by one. The last observation is indeed expected, by considering the fading of the channel.

Fig. 5b depicts the outage probability $P_{M,N}^{\text{out}}$ for the multiplexing mode in (26) versus the average system transmit SNR P_T/N_0 . The following can be observed: with every additional BS the outage probability increases. This observation is indeed expected, since the transmit power decreases for each BS with every additional BS.

Fig. 6a depicts the exact and approximated system throughput $T_{D,N}$ for the diversity mode in (45) and (46), respectively,

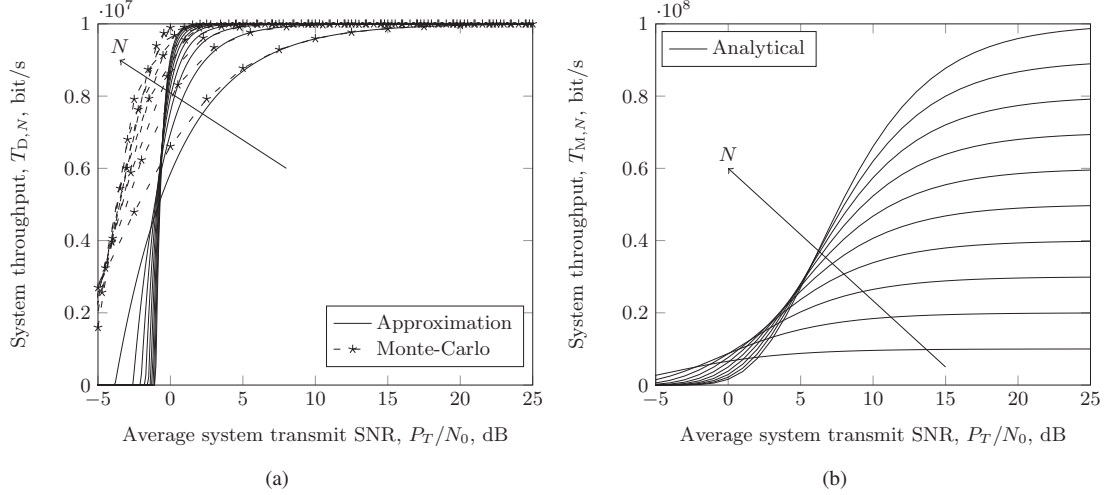


Fig. 6: Exact and approximated system throughput with $N = 1, 2, \dots, 10$ for (a) diversity mode and (b) multiplexing mode.

versus the average system transmit SNR P_T/N_0 . The following can be observed: (i) with every additional BS the maximum system throughput of $T_{D,N,\max} = 10$ Mbit/s can be reached at a lower SNR; (ii) the maximum system throughput does not increase with additional BSs, since identical sequences are transmitted; and (iii) the approximation at low SNR reveals a mismatch.

Fig. 6b depicts the system throughput $T_{M,N}$ for the multiplexing mode in (47) versus the average system transmit SNR P_T/N_0 . The following can be observed: (i) at low SNR few BSs achieve a higher system throughput whereas at high SNR many BSs achieve a higher system throughput; and (ii) the maximum system throughput is $T_{M,N,\max} = N \cdot 10$ Mbit/s, and thus increases with every additional BS.

Remark: As illustrated in Fig. 5a and Fig. 6a we have a mismatch of the diversity mode approximation at low SNR. For the performance comparison and the DMT we adjust the approximated outage probability in (18). That the adjustment is reasonable shall become apparent in the next paragraph.

Fig. 7 depicts the exact and approximated outage probability $P_{D,N}^{\text{out}}$ for the diversity mode for JD in (16) and (18), respectively,

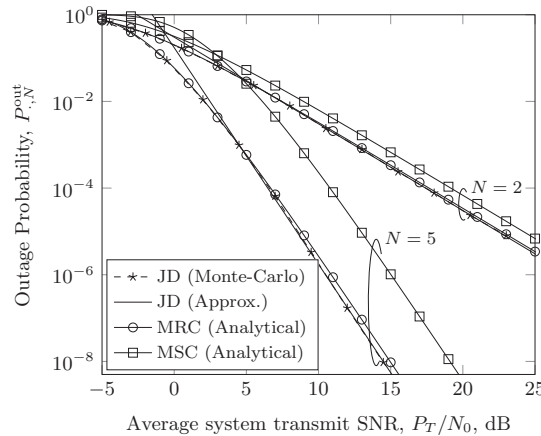


Fig. 7: Outage probability for JD, MRC and MSC with $N \in \{2, 5\}$.

and the outage probability for MSC $P_{\text{MSC},N}^{\text{out}}$ in (32), and for MRC $P_{\text{MRC},N}^{\text{out}}$ in (41), versus the average system transmit SNR P_T/N_0 . We show results for different numbers of BSs, i.e., $N \in \{2, 5\}$. The following can be observed: (i) JD outperforms

MSR and MRC, and (ii) the outage probabilities of JD and MRC are close at low SNR. Based on the last observation, we make use of the closed-form expression in (41) to adjust the approximation in (18), i.e.,

$$P_{D,N}^{\text{out}} \approx \min \left(\frac{A_N}{\bar{\Gamma}_1 \bar{\Gamma}_2 \dots \bar{\Gamma}_N}, 1 - \exp \left(-\frac{A_1}{\bar{\Gamma}_1} \right) \cdot \left(\sum_{i=1}^N \frac{(A_1/\bar{\Gamma}_i)^{(i-1)}}{(i-1)!} \right) \right), \quad (51)$$

for $\bar{\Gamma}_1 = \dots = \bar{\Gamma}_N = \bar{\Gamma}_i$. We can use the min-operation, since we know that MRC is suboptimal in comparison to JD [17], such that the JD outage probability is less or equal to the MRC outage probability. In the following the outage probability and system throughput for the diversity mode is assessed based on (51).

Fig. 8a, Fig. 8b and Fig. 8c depict the required average system transmit SNR $P_T/N_0 = \sigma_i(P_*^{\text{out}})$ to achieve the target outage

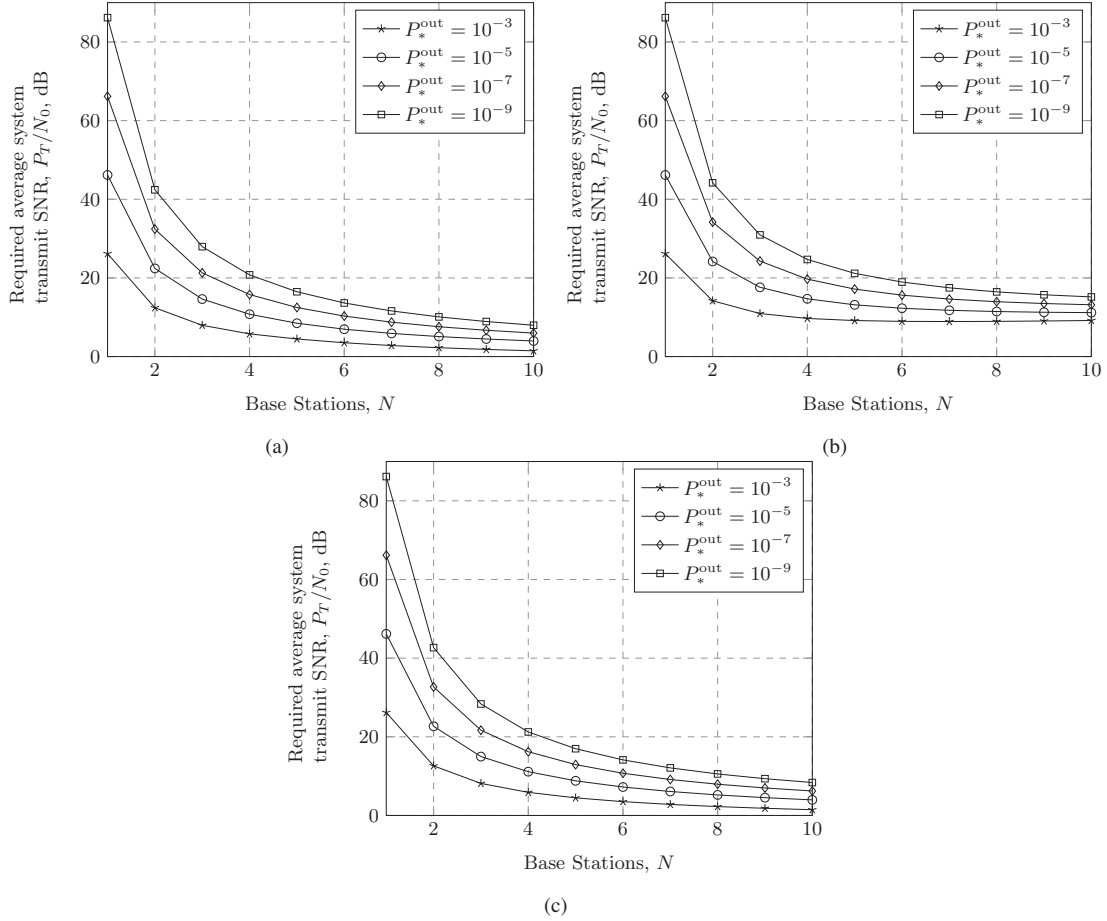


Fig. 8: Required average system transmit SNR for target outage probability for (a) JD, (b) MSC, and (c) MRC.

probability for JD, MSC and MRC, respectively, given in (42), versus the number of BSs. The following can be observed: (i) for JD and MRC to achieve a targeted outage probability the required average system transmit SNR decreases with an increase of BSs; and (ii) for MSC an optimal number of BSs exists to minimize the required average system transmit SNR for a targeted outage probability. The last observation can be reasoned by the fact that an increasing numbers of BSs yield a diversity order increase but simultaneously decreases the transmit power per BS. A similar study of optimal operating points for MSC can be found in [30].

Fig. 9a and Fig. 9b depict the SNR gain of JD $G_{JD,i}$ in comparison to MSC and MRC, respectively, given in (43), versus the number of BSs. The following can be observed: (i) JD outperforms MSC and MRC; (ii) for MSC, with every additional BS the SNR gain increases; and (iii) for MRC, a maximum exists which depends on the number of BSs and targeted outage probability. The last observation can be reasoned by considering the outage probability of JD and MRC at low SNR. If the number of BS increases, less average system transmit SNR is required, i.e., the system approaches low SNR regime. As observed in Fig. 7 the outage probability of JD and MRC come close at low SNR.

Fig. 10a, Fig. 10b and Fig. 10c depict the DMT in (50) for different average system transmit SNRs, numbers of BSs and spectral efficiencies, respectively. The outage probability is depicted versus the system throughput. The graphs are generated as follows: (i) if $\alpha = 1.0$, we achieve full diversity (diversity mode) which leads to a low outage probability at the cost of a low system throughput; (ii) if $\alpha = 0.0$, we achieve full multiplexing (multiplexing mode) which leads to a high system throughput

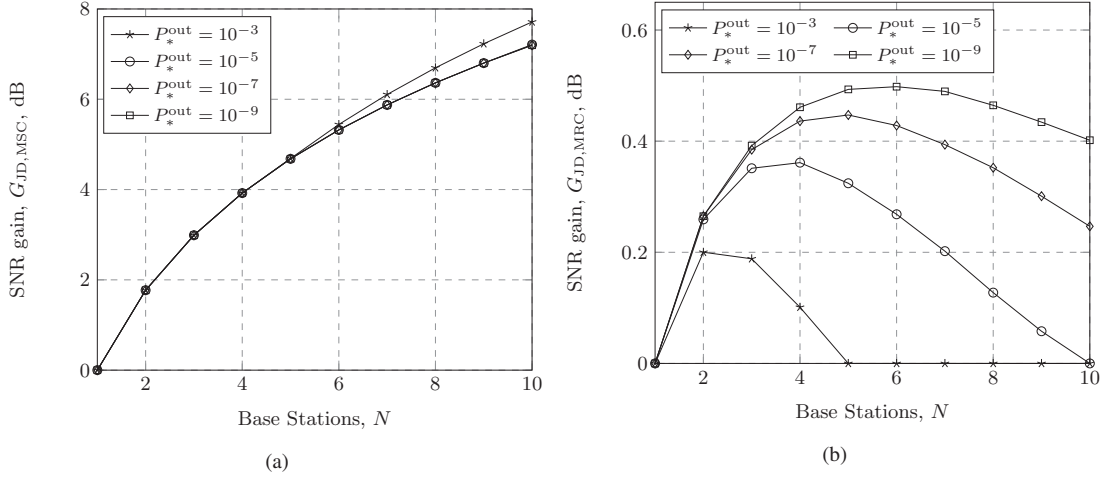


Fig. 9: Gain of required average system transmit SNR for target outage probability for (a) MSC and (b) MRC.

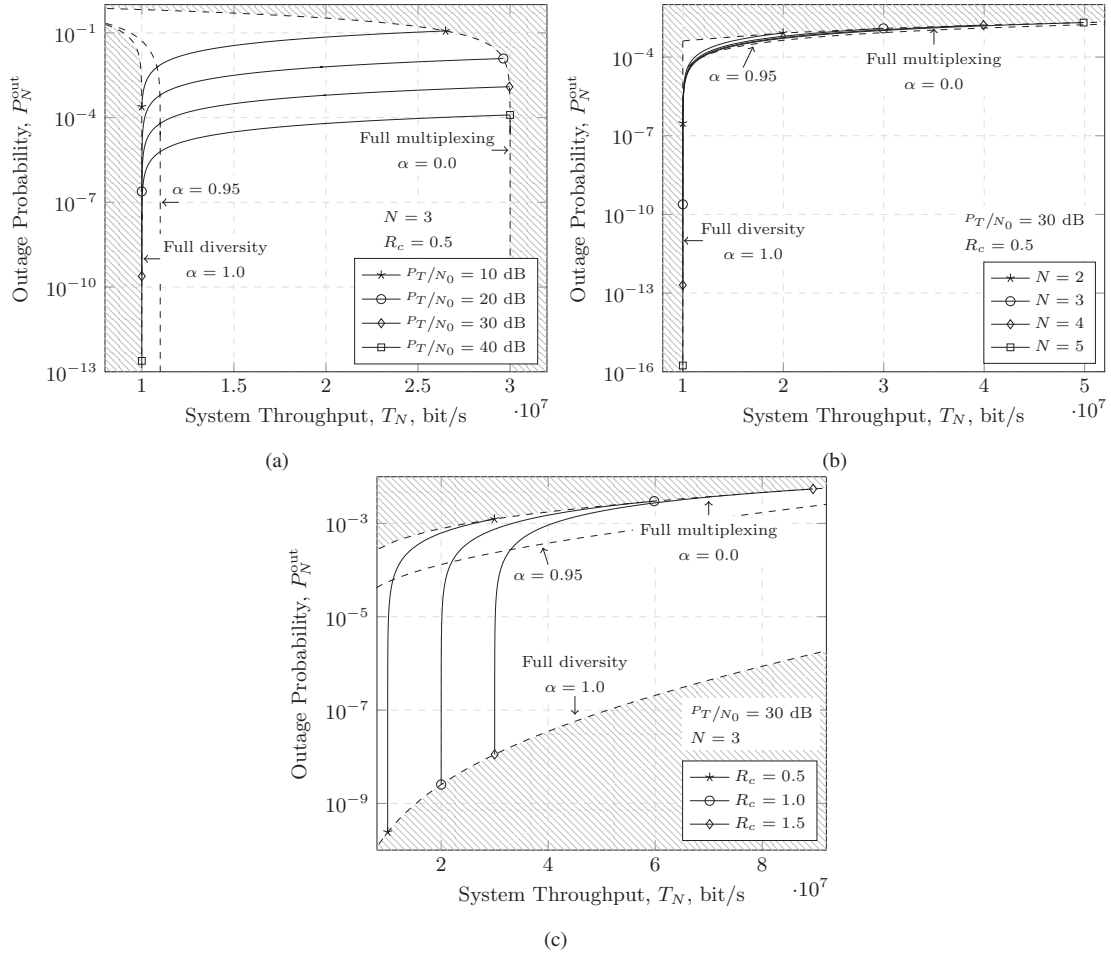


Fig. 10: Diversity-multiplexing tradeoff for different (a) average system transmit SNRs, (b) number of BSs, and (c) spectral efficiencies; the infeasible region is depicted as shaded area.

at the cost of a high outage probability; and (iii) if $0.0 < \alpha < 1.0$, the outage probability and system throughput are achieved by time sharing between both modes. We depicted for both corner cases (full multiplexing and full diversity) all achievable pairs of the outage probability and the system throughput for any value of the parameter under investigation (average system transmit SNR, number of BSs and spectral efficiency) by dashed lines. The shaded area cannot be reached for any time sharing setting and any value of the parameter under investigation. This area is referred to as the infeasible region. In addition, we depicted the time sharing for $\alpha = 0.95$ by a dashed line.

Fig. 10a depicts the DMT for different average system transmit SNRs with $N = 3$. The following can be observed: (i) with an increase of the average system transmit SNRs the DMT curve shifts towards lower outage probability and higher system throughput; and (ii) the system throughput is upper bounded by $T_{\max} = 30$ Mbit/s such that it does not increase for average system transmit SNRs $P_T/N_0 \geq 30$ dB.

Fig. 10b depicts the DMT for different number of BSs with $P_T/N_0 = 30$ dB. The following can be observed: with an increase of the number of BSs the DMT curve stretches towards lower outage probability and higher system throughput.

Fig. 10c depicts the DMT for different spectral efficiencies with $P_T/N_0 = 30$ dB and $N = 3$. The following can be observed: with an increase of the spectral efficiency the DMT curve shifts towards higher outage probability and higher system throughput.

For the DMT analysis, the slope $|\Delta T_N|/|\Delta P_N^{\text{out}}|$ is of interest. We observe two different slope regions:

Region 1: If we operate around point $\alpha = 0.95$, an incremental change $|\Delta \alpha|$ provokes rather balanced incremental changes $|\Delta T_N|$ and $|\Delta P_N^{\text{out}}|$, but the system throughput and outage probability around point $\alpha = 0.95$ is rather poor in comparison to the maximum achievable values at point $\alpha = 0.0$ (full multiplexing) or point $\alpha = 1.0$ (full diversity).

Region 2: If we operate around point $\alpha = 0.0$ or $\alpha = 1.0$, an incremental change $|\Delta \alpha|$ provokes rather unbalanced incremental change $|\Delta T_N|$ and $|\Delta P_N^{\text{out}}|$, but the network can achieve either high system throughput (full multiplexing) or low outage probabilities (full diversity).

As depicted in Fig. 10 the DMT analysis depends on multiple parameters, such as the modulation scheme, the code rate, the bandwidth, the number of communication links and the transmit power. So it is important for the network to find a suitable point of operation.

IX. CELLULAR FIELD TRIAL FOR UPLINK

In [31] measurements were carried out in a field trial testbed in Dresden (Germany) downtown. We make use of this measurement data to show the potential of MC in a real cellular network. In the field trial the uplink was considered. In this section, we shortly introduce the field trial setup and then present the empirical outage probability cumulative distribution function (CDF) for the measurement data. Our results elaborate on the following points: (i) the performance improvement if multiple links are included in the transmission and (ii) the performance gain of JD in comparison to MSC and MRC.

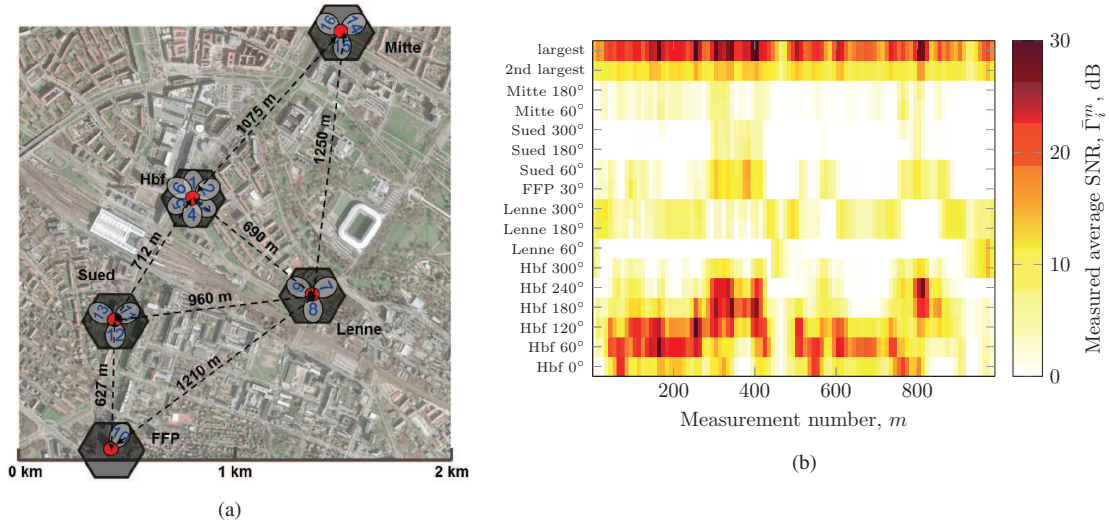


Fig. 11: (a) Testbed deployment and (b) measured average SNR $\bar{\Gamma}_i^m$ achieved at all BSs of the testbed during the complete field trial [31].

A. Field Trial Setup

The field trial testbed, deployed in downtown Dresden, is depicted in Fig. 11a. In total, 16 BSs located on five sites with up to six-fold sectorization are used for the measurements. Each BS is equipped with a two element, cross-polarized KATHREIN 80010541 antenna. The basic physical layer procedures are used in close compliance with the 3GPP/LTE standard (see e.g. [32]). During the field trial, two UEs were moved on a measurement bus in 5 m distance while transmitting on the same time and frequency resources employing one dipole antenna each. The superimposed signal is jointly received by all BSs which took snapshots of 80 ms (corresponding to 80 transmit time intervals (TTIs)) every 10 s. In total about 1900 such measurements were taken in order to observe a large number of different transmission scenarios. In Fig. 11b the measured average SNR $\bar{\Gamma}_i^m$ values for around 1000 measurements observed at all BSs and locations are shown, where m denotes the measurement number and i the BS index, $i \in \{\text{Hbf } 0^\circ, \text{Hbf } 60^\circ, \dots\}$. The two largest average SNRs measured at any BS for each measurement are depicted in the upper part of the figure. An interesting result is that multiple relatively high average SNR values of two

different BSs are observed at each location of the UEs. Since JD is particularly beneficial in scenarios with multiple relatively high average SNR values, the result indicates that cooperation among BSs can improve reliable data transmission as presented in the next section. For more details on this field trial setup, please refer to [31].

B. Empirical Outage Probability CDF

With the measured average SNR $\bar{\Gamma}_i^m$ in Fig. 11b we can generate an empirical outage probability CDF for the diversity mode. For each measurement we consider the strongest links, i.e., the largest measured average SNRs $\bar{\Gamma}_i^m$. The outage probability can be assessed with (51), (32) and (40) for JD, MSC and MRC, respectively, for each measurement. For MRC we have to calculate the pdf of the received SNR Γ_{MRC} in (35), since the results in (36) holds iff the average SNRs $\bar{\Gamma}_i$ are equal. The pdf in (35) for the received SNR Γ_{MRC} with $N = 2$ and $N = 3$ is

$$f_{\Gamma_{\text{MRC}}}(\gamma_{\text{MRC}}) = \frac{\exp\left(-\frac{\gamma_{\text{MRC}}}{\bar{\Gamma}_1}\right)}{\bar{\Gamma}_1 - \bar{\Gamma}_2} + \frac{\exp\left(-\frac{\gamma_{\text{MRC}}}{\bar{\Gamma}_2}\right)}{\bar{\Gamma}_2 - \bar{\Gamma}_1} \quad (52)$$

and

$$f_{\Gamma_{\text{MRC}}}(\gamma_{\text{MRC}}) = \frac{\bar{\Gamma}_1 \exp\left(-\frac{\gamma_{\text{MRC}}}{\bar{\Gamma}_1}\right)}{(\bar{\Gamma}_1 - \bar{\Gamma}_2)(\bar{\Gamma}_1 - \bar{\Gamma}_3)} + \frac{\bar{\Gamma}_2 \exp\left(-\frac{\gamma_{\text{MRC}}}{\bar{\Gamma}_2}\right)}{(\bar{\Gamma}_2 - \bar{\Gamma}_1)(\bar{\Gamma}_2 - \bar{\Gamma}_3)} + \frac{\bar{\Gamma}_3 \exp\left(-\frac{\gamma_{\text{MRC}}}{\bar{\Gamma}_3}\right)}{(\bar{\Gamma}_3 - \bar{\Gamma}_1)(\bar{\Gamma}_3 - \bar{\Gamma}_2)}, \quad (53)$$

respectively. By substituting (52) and (53) into (40) we can numerically calculate the outage probability for MRC. We then generate the empirical outage probability CDF for JD, MSC and MRC with all measured average SNRs.

Fig. 12 depicts the empirical outage probability CDF for the diversity mode for different number of BSs with JD, MSC and MRC. The following can be observed: (i) with an increasing number of BSs the outage probability decreases; (ii) JD outperforms MSC and MRC; and (iii) with additional BSs the performance gain of JD increases. The observations are indeed expected, as discussed in Section V and Section VIII.

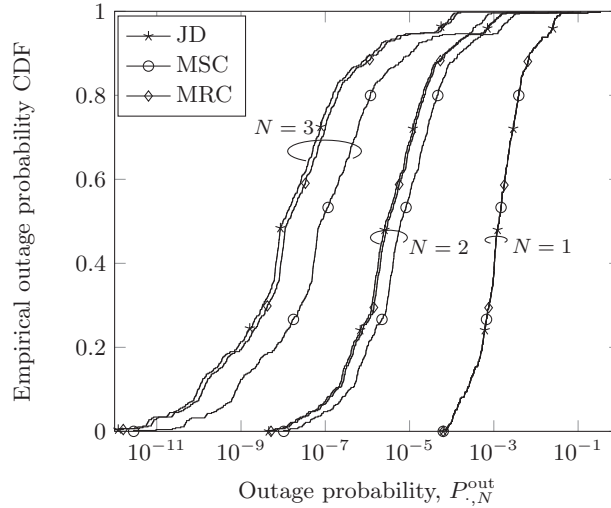


Fig. 12: Empirical outage probability CDF ($N = 1, 2, 3$) for JD, MSC and MRC.

C. Discussion

Based on the field trial setup, we can conclude that MC can achieve a substantial performance improvement in real cellular networks. The measurement data at hand documents that multiple relatively high average SNR values frequently occur in which JD is particularly beneficial. From the uplink measurement data we can also draw conclusions for the downlink. As argued in Section II-B the statistical properties of the link model are identical for the up- and downlink. Thus, if the measurement data at hand documents that multiple relatively high average SNR values frequently occur in the uplink, it is reasonable to assume that multiple relatively high average SNR values frequently occur in the downlink as well. Based on this insight, MC can achieve low outage probabilities or high system throughput in real cellular networks considering the downlink. In dependency on the user requirements, our DMT analysis allows the network to adjust the system configurations.

X. CONCLUSION

In this work we have investigated multi-connectivity architectures and have shown that enhanced data rates or high transmission reliability can be achieved. To evaluate the performance gain of multi-connectivity we have analytically described the outage probability and the system throughput based on distributed source coding. We have achieved a remarkably simple, yet accurate analytical framework to describe the relation of the outage probability and the system throughput in dependency on the number of links, the modulation scheme, the code rate, the bandwidth, and the received SNR. We have established a diversity-multiplexing tradeoff analysis to investigate the tradeoff between low outage probabilities and high system throughput based on time sharing between the diversity mode and the multiplexing mode. In the diversity mode, which aims for low outage probabilities, we showed the SNR reduction of joint decoding in comparison to maximum selection combining and maximum ratio combining while achieving the same outage probability. On the other hand, the multiplexing mode aims to achieve high system throughput. The diversity-multiplexing tradeoff analysis allows the network to adjust the system configurations accordingly to the user requirements. In addition, we have applied the analytical framework to real cellular networks. Based on the measurement data recorded in a field trial testbed in an urban region we have evaluated the possible performance improvement by the use of MC. The measurement data document that multiple relatively high average SNR values frequently occur in which MC is particularly beneficial.

APPENDIX A

APPROXIMATED OUTAGE PROBABILITY FOR THE DIVERSITY MODE

The approximated outage probability for the diversity mode can be obtained as

$$P_{D,N}^{\text{out}} = \int_{\gamma_1=0}^{2^{R_c}-1} \int_{\gamma_2=0}^{2^{R_c-\phi(\gamma_1)}-1} \dots \int_{\gamma_N=0}^{2^{R_c-\phi(\gamma_1)-\phi(\gamma_2)-\dots-\phi(\gamma_{N-1})}-1} \frac{1}{\bar{\Gamma}_1} \exp\left(-\frac{\gamma_1}{\bar{\Gamma}_1}\right) \frac{1}{\bar{\Gamma}_2} \exp\left(-\frac{\gamma_2}{\bar{\Gamma}_2}\right) \dots \frac{1}{\bar{\Gamma}_N} \exp\left(-\frac{\gamma_N}{\bar{\Gamma}_N}\right) d\gamma_N \dots d\gamma_2 d\gamma_1 \quad (54)$$

$$\approx \int_{\gamma_1=0}^{2^{R_c}-1} \int_{\gamma_2=0}^{2^{R_c-\phi(\gamma_1)}-1} \dots \int_{\gamma_N=0}^{2^{R_c-\phi(\gamma_1)-\phi(\gamma_2)-\dots-\phi(\gamma_{N-1})}-1} \frac{1}{\bar{\Gamma}_1} \left(1 - \frac{\gamma_1}{\bar{\Gamma}_1}\right) \frac{1}{\bar{\Gamma}_2} \left(1 - \frac{\gamma_2}{\bar{\Gamma}_2}\right) \dots \frac{1}{\bar{\Gamma}_N} \left(1 - \frac{\gamma_N}{\bar{\Gamma}_N}\right) d\gamma_N \dots d\gamma_2 d\gamma_1 \quad (55)$$

$$\approx \frac{1}{\bar{\Gamma}_1 \bar{\Gamma}_2 \dots \bar{\Gamma}_N} \int_{\gamma_1=0}^{2^{R_c}-1} \int_{\gamma_2=0}^{2^{R_c-\phi(\gamma_1)}-1} \dots \int_{\gamma_N=0}^{2^{R_c-\phi(\gamma_1)-\phi(\gamma_2)-\dots-\phi(\gamma_{N-1})}-1} 1 d\gamma_N \dots d\gamma_2 d\gamma_1 \quad (56)$$

$$= \frac{A_N}{\bar{\Gamma}_1 \bar{\Gamma}_2 \dots \bar{\Gamma}_N}, \quad (57)$$

The steps are justified as follows: (54) is the substitution of the pdf $f(\gamma_i)$ given in (4) into (16); (55) MacLaurin series for exponential function $\exp(-x_i) \approx 1 - x_i$ for $x_i \rightarrow 0$, (56) expanding the resulting product as $\prod_i (1 - x_i) \approx 1$ for $x_i \rightarrow 0$; (57) is proven in Theorem 3 and the assumption that the received SNRs are independently distributed, thus we can interchange the integral bounds.

Theorem 3 For any $N \in \mathbb{N} \setminus \{1\}$,

$$A_N(x) = \int_{\gamma_N=0}^{2^x-1} \int_{\gamma_{N-1}=0}^{2^{x-\phi(\gamma_N)}-1} \dots \int_{\gamma_1=0}^{2^{x-\phi(\gamma_N)-\dots-\phi(\gamma_2)}-1} 1 d\gamma_1 \dots d\gamma_{N-1} d\gamma_N \quad (58)$$

$$= (-1)^N + 2^x \sum_{n=0}^{N-1} (-1)^{N+n+1} \frac{1}{n!} x^n (\ln(2))^n. \quad (59)$$

Proof Base case: If $N = 2$, then (58) is

$$A_2(x) = \int_{\gamma_2=0}^{2^x-1} \int_{\gamma_1=0}^{2^{x-\phi(\gamma_2)}-1} 1 d\gamma_1 d\gamma_2 \quad (60)$$

$$= \int_{\gamma_2=0}^{2^x-1} \left[\frac{2^x}{1 + \gamma_2} - 1 \right] d\gamma_2 \quad (61)$$

$$= 2^x (x \cdot \ln(2) - 1) + 1, \quad (62)$$

which is (59) for $N = 2$. So, the theorem holds for $N = 2$.

Inductive hypothesis: Suppose the theorem holds for all values of N up to some $K \geq 2$.

Inductive step: Let $N = K + 1$, then (58) is

$$A_{K+1}(x) = \int_{\gamma_{K+1}=0}^{2^x-1} \underbrace{\int_{\gamma_K=0}^{2^{x-\phi(\gamma_{K+1})}-1} \dots \int_{\gamma_1=0}^{2^{x-\phi(\gamma_{K+1})-\dots-\phi(\gamma_2)-1}} 1 d\gamma_1 \dots d\gamma_K d\gamma_{K+1}}_{A_K(x-\phi(\gamma_{K+1}))} \quad (63)$$

$$= \int_{\gamma_{K+1}=0}^{2^x-1} \left[(-1)^K + \frac{2^x}{1+\gamma_{K+1}} \sum_{n=0}^{K-1} (-1)^{K+n+1} \frac{1}{n!} (x - \phi(\gamma_{K+1}))^n (\ln(2))^n \right] d\gamma_{K+1} \quad (64)$$

$$= \int_{\gamma_{K+1}=0}^{2^x-1} \left[(-1)^K + \frac{2^x}{1+\gamma_{K+1}} \sum_{n=0}^{K-1} (-1)^{K+n+1} \frac{1}{n!} (\ln(2))^n \cdot \sum_{k=0}^n (-1)^k \binom{n}{k} x^{n-k} \phi(\gamma_{K+1})^k \right] d\gamma_{K+1} \quad (65)$$

$$= (-1)^K \gamma_{K+1} + 2^x \sum_{n=0}^{K-1} (-1)^{K+n+1} \frac{1}{n!} (\ln(2))^n \cdot \sum_{k=0}^n (-1)^k \binom{n}{k} x^{n-k} \frac{(\ln(1+\gamma_{K+1}))^{k+1}}{(k+1)(\ln(2))^k} \Bigg|_{\gamma_{K+1}=0}^{2^x-1} \quad (66)$$

$$= (-1)^K 2^x + (-1)^{K+1} + 2^x \sum_{n=0}^{K-1} (-1)^{K+n+1} \frac{1}{n!} x^{n+1} (\ln(2))^{n+1} \underbrace{\sum_{k=0}^n (-1)^k \binom{n}{k} \frac{1}{k+1}}_{\frac{1}{n+1}} \quad (67)$$

$$= (-1)^{K+1} + 2^x \sum_{n=0}^K (-1)^{K+n} \frac{1}{n!} x^n (\ln(2))^n. \quad (68)$$

The steps are justified as follows: (64) is our inductive hypothesis; for (65) we have used the binomial formula; (68) we have used the following

$$\sum_{k=0}^n (-1)^k \binom{n}{k} \frac{1}{k+1} = \frac{1}{n+1} \sum_{k=0}^n (-1)^k \binom{n+1}{k+1} \quad (69)$$

$$= \frac{-1}{n+1} \underbrace{\left[\sum_{k=1}^{n+1} (-1)^k \binom{n+1}{k} + \binom{n+1}{0} - \binom{n+1}{0} \right]}_{\sum_{k=0}^{n+1} (-1)^k \binom{n+1}{k} = (1-1)^{n+1} = 0} = \frac{1}{n+1} \quad (70)$$

and carried out some algebraic manipulations. Equation (68) corresponds to (59) for $N = K + 1$. So, the theorem holds for $N = K + 1$. Hence, by the principle of mathematical induction, the theorem holds for all $N \in \mathbb{N} \setminus \{1\}$. ■

REFERENCES

- [1] A. Wolf, P. Schulz, D. Öhmann, M. Dörpinghaus, and G. Fettweis, "Diversity-multiplexing tradeoff for multi-connectivity," in *preparation for submission to IEEE Globecom (GC)*, Singapur, Dec. 2017.
- [2] —, "On the gain of joint decoding for multi-connectivity," in *preparation for submission to IEEE Globecom (GC)*, Singapur, Dec. 2017.
- [3] M. Eriksson, "Dynamic single frequency networks," *IEEE Journal on Selected Areas in Communications*, vol. 19, no. 10, pp. 1905–1914, Oct. 2001.
- [4] P. Marsch and G. P. Fettweis, *Coordinated Multi-Point in Mobile Communications: from Theory to Practice*. Cambridge University Press, 2011.
- [5] 3GPP, "Coordinated multi-point operation for LTE physical layer aspects," TR 36.819 V11.1.0, 2011.
- [6] A. Ravanshid, P. Rost, D. S. Michalopoulos, V. V. Phan, H. Bakker, D. Aziz, S. Tayade, H. D. Schotten, S. Wong, and O. Holland, "Multi-connectivity functional architectures in 5G," in *Proc. IEEE International Conference on Communications Workshops (ICCW)*, Kuala Lumpur, Malaysia, May 2016, pp. 187–192.
- [7] Nokia, "5G for mission critical communication: Achieve ultra-reliability and virtual zero latency," *White paper*, 2016.
- [8] E. Dahlman, S. Parkvall, and J. Skold, *4G, LTE-Advanced Pro and The Road to 5G*. Academic Press, 2016.
- [9] D. S. Michalopoulos, I. Viering, and L. Du, "User-plane multi-connectivity aspects in 5G," in *Proc. IEEE 23rd International Conference on Telecommunications (ICT)*, Thessaloniki, Greece, May 2016, pp. 1–5.
- [10] G. Pocovi, B. Soret, M. Lauridsen, K. I. Pedersen, and P. Mogensen, "Signal quality outage analysis for ultra-reliable communications in cellular networks," in *Proc. IEEE Globecom Workshops (GCW)*, San Diego, USA, Dec. 2015, pp. 1–6.
- [11] F. B. Tesema, A. Awada, I. Viering, and G. P. Fettweis, "Mobility modeling and performance evaluation of multi-connectivity in 5G intra-frequency networks," in *Proc. IEEE Globecom Workshops (GCW)*, San Diego, USA, Dec. 2015, pp. 1–6.

- [12] J. J. Nielsen and P. Popovski, "Latency analysis of systems with multiple interfaces for ultra-reliable M2M communication," in *Proc. IEEE 17th International Workshop on Signal Processing Advances in Wireless Communications (SPAWC)*, Edinburgh, UK, Jul. 2016, pp. 1–6.
- [13] L. Zheng and D. N. C. Tse, "Diversity and multiplexing: a fundamental tradeoff in multiple-antenna channels," *IEEE Trans. Inf. Theory*, vol. 49, no. 5, pp. 1073–1096, May 2003.
- [14] D. N. C. Tse, P. Viswanath, and L. Zheng, "Diversity-multiplexing tradeoff in multiple-access channels," *IEEE Trans. Inf. Theory*, vol. 50, no. 9, pp. 1859–1874, Sept. 2004.
- [15] R. Narasimhan, "Finite-SNR diversity-multiplexing tradeoff for correlated rayleigh and rician MIMO channels," *IEEE Trans. Inf. Theory*, vol. 52, no. 9, pp. 3965–3979, Sept. 2006.
- [16] E. Stauffer, O. Oyman, R. Narasimhan, and A. Paulraj, "Finite-SNR diversity-multiplexing tradeoffs in fading relay channels," *IEEE Journal on Selected Areas in Communications*, vol. 25, no. 2, pp. 245–257, Feb. 2007.
- [17] A. F. Molisch, *Wireless Communications*. John Wiley & Sons, 2012.
- [18] D. Brennan, "Linear diversity combining techniques," *Proceedings of the IRE*, vol. 47, no. 6, pp. 1075–1102, 1959.
- [19] D. Slepian and J. Wolf, "Noiseless coding of correlated information sources," *IEEE Trans. Inf. Theory*, vol. 19, no. 4, pp. 471–480, Jul. 1973.
- [20] M. Cheng, K. Anwar, and T. Matsumoto, "Outage probability of a relay strategy allowing intra-link errors utilizing Slepian-Wolf theorem," *EURASIP J. Adv. Signal Process*, vol. 2013, no. 1, pp. 1–12, Feb. 2013.
- [21] X. Zhou, M. Cheng, X. He, and T. Matsumoto, "Exact and approximated outage probability analyses for decode-and-forward relaying system allowing intra-link errors," *IEEE Trans. Wireless Commun.*, vol. 13, no. 12, pp. 7062–7071, Dec. 2014.
- [22] A. El Gamal and Y.-H. Kim, *Network Information Theory*. Cambridge: Cambridge University Press, 2011.
- [23] D. C. Gonzalez, A. Wolf, L. L. Mendes, J. C. S. S. Filho, and G. Fettweis, "An efficient power allocation scheme for multirelay systems with lossy intra-links," *IEEE Trans. Commun.*, vol. 65, no. 4, pp. 1–12, Apr. 2017.
- [24] A. Goldsmith, *Wireless Communications*. Cambridge University Press, 2005.
- [25] B. Van Laethem, F. Quitin, F. Bellens, C. Oestges, and P. De Doncker, "Correlation for multi-frequency propagation in urban environments," *Progress In Electromagnetics Research Letters*, vol. 29, pp. 151–156, 2012.
- [26] X. He, "Binary information sensing and multiterminal source coding: Rate-distortion analysis and transmission design," Ph.D. dissertation, JAIST, Japan, 2016.
- [27] T. Cover, "A proof of the data compression theorem of Slepian and Wolf for ergodic sources (corresp.)," *IEEE Trans. Inf. Theory*, vol. 21, no. 2, pp. 226–228, Mar. 1975.
- [28] T. M. Cover and J. A. Thomas, *Elements of information theory*, 2nd ed. Hoboken, NJ: Wiley-Interscience, 2006.
- [29] T. M. Duman and A. Ghayeb, *Coding for MIMO Communication Systems*. John Wiley & Sons, 2008.
- [30] D. Öhmann, M. Simsek, and G. P. Fettweis, "Achieving high availability in wireless networks by an optimal number of Rayleigh-fading links," in *Proc. IEEE Globecom Workshops (GCW)*, Austin, TX, USA, Dec. 2014, pp. 1402–1407.
- [31] M. Grieger, "Uplink joint detection in a realistic macro cellular environment," Ph.D. dissertation, TU Dresden, Germany, 2014.
- [32] 3GPP, "Further advancements for E-UTRA: Physical layer aspects," TR 36.814 v9.0.0, Mar. 2010.